Quantum simulation of conductivity plateaux and fractional quantum Hall effect using ultracold atoms

Nuria Barberán[1]**, Daniel Dagnino**[2]**, Miguel Angel García-March**[1,3]**,**
Andrea Trombettoni[4,5]**, Josep Taron**[1,6]**, Maciej Lewenstein**[3,7]

[1]Departament d'Estructura i Constituents de la Matèria, Facultat de Física, Universitat de Barcelona, Diagonal 645, E-08028 Barcelona, Spain
[2]Barcelona Center for Subsurface Imaging, Institute of Marine Sciences, CSIC, Pg. Marítim de la Barceloneta 37-49, 08003 Barcelona, Spain
[3]ICFO-Institut de Ciències Fotòniques, The Barcelona Institute of Science and Technology, 08860 Castelldefels (Barcelona), Spain
[4]CNR-IOM DEMOCRITOS Simulation Center, Via Bonomea 265, I-34136 Trieste, Italy
[5]SISSA and INFN, Sezione di Trieste, Via Bonomea 265, I-34136 Trieste, Italy
[6]Institut de Ciències del Cosmos, E-08028 Barcelona, Spain.
[7]ICREA-Institució Catalana de Recerca i Estudis Avançats, 08010 Barcelona, Spain

Abstract.
We analyze the role of impurities in the fractional quantum Hall effect using a highly controllable system of ultracold atoms. We investigate the mechanism responsible for the formation of plateaux in the resistivity/conductivity as a function of the applied magnetic field in the lowest Landau level regime. To this aim, we consider an impurity immersed in a small cloud of an ultracold quantum Bose gas subjected to an artificial magnetic field. We consider scenarios corresponding to experimentally realistic systems with gauge fields induced by rotation of the trapping parabolic potential. Systems of this kind are adequate to simulate quantum Hall effects in ultracold atom setups. We use exact diagonalization for few atoms and, to emulate transport equations, we analyze the time evolution of the system under a periodic perturbation. We provide a theoretical proposal to detect the up-to-now elusive presence of strongly correlated states related to fractional filling factors in the context of ultracold atoms. We analyze the conditions under which these strongly correlated states are associated with the presence of the resistivity/conductivity plateaux. Our main result is the presence of a plateau in a region, where the transfer between localized and non-localized particles takes place, as a necessary condition to maintain a constant value of the resistivity/conductivity as the magnetic field increases.

1. Introduction

Transport properties provide some of the most fundamental characteristics of condensed matter systems (cf. [1, 2]). In contrast, in physics of ultracold atomic and molecular gases [3], the studies of transport, unlike those performed in solid state settings, are hindered by the difficulty of having continuous and durable flow of atoms; for this reason they have been very limited so far. Among others they included: the investigations of Bloch oscillations (from the early studies with cold atoms [4] to the recent experiments with disordered gases [5]), the extensive work on transport and diffusion in disordered gases [6, 7, 8, 9, 10], and the very recent experiments on quantized conductivity [11, 12, 13, 14, 15].

Paradigmatic systems, in which the transport properties play an essential role, are the systems that exhibit integer or fractional quantum Hall effects (IQHE, or FQHE) [16, 17]. The quantum Hall effect consists in fact in *quantisation of the transverse conductance* for electronic current in the condensed matter systems, and for atomic flow for neutral atomic gases. Although in the IQHE the interactions play an irrelevant role, the underlying physics, even if well understood, is highly non-trivial. The case of the FQHE, where the interaction has a crucial contribution, is more complex and not yet completely understood. For these reasons systems that exhibit FQHE belong to the most popular systems of strongly correlated particles that still await conclusive explanations and "call for" quantum simulations, for instance with ultracold atoms or ions [3].

In order to quantum simulate QHE it is necessary to generate strong artificial magnetic (gauge) fields. In the context of ultracold atomic systems, first realizations of artificial gauge (magnetic) fields were considered in rotating traps [18, 19, 20, 21, 22, 23, 24]. Quite soon it was realized, however, that the most promising way to generate the artificial gauge fields is to use the laser induced fields – these methods are described in detail in several reviews [3, 25, 26, 27], while for the recent spectacular experiments the reader should consult cf. [28, 29, 30, 31]. Various methods of detection of the Hall effect have been proposed and realized in the mentioned experiments (see cf. [32, 33]). In particular, it was shown [34] how the quantized Hall conductance can be measured from density profiles using the Středa formula [35]. In this paper we propose to measure the quantized Hall conductance directly as a transport property and suggest to use the response of the considered system to the time dependent perturbation.

Before we turn to atomic systems, it is instructive to review briefly the phenomenology of electronic systems [16, 36]. Hall effect appears already in classical physics, where the transverse resistivity is proportional to the magnetic field B. The transverse conductivity may be expressed by the famous expression

$$\sigma_{yx} = \nu \frac{e^2}{h},$$

(1)

where $\nu = nh/eB$ is the filling factor, and n is the electron areal density. Amazingly the same formula holds in the quantum mechanical case, being the consequence of the Galilean invariance [36].

The explanation of plateaux corresponding to integer filling factors observed in

experiments requires thus additional arguments. These arguments are based on the fact that in typical experimental situations Galilean invariance breaks down due to the presence of random impurities. Accordingly, the spectrum of (non-interacting) 2D electron gas in the magnetic field does not exhibit discrete Landau levels only. Close to the Landau levels in fact the spectrum consists of a band corresponding to extended (conducting) states. Far from the Landau level energy the spectrum corresponds to states localized due to the presence of impurities via the mechanism of Anderson localization [37]. Obviously, localized states do not contribute to the conductivity, and thus one can expect that when Fermi energy decreases between two subsequent Landau levels including less and less localized states in the Fermi sea, keeping the condition of fully occupied Landau levels, the conductivity does not change i.e. it exhibits a plateau. Why has the plateau the value exactly equal to $\sigma_{yx} = \nu \frac{e^2}{h}$ with ν integer, and why is this result so robust was a rather surprising fact in the beginning of the 1980s. It was first explained by the famous Laughlin argument [38]. He demonstrated the quantization of the Hall resistivity analyzing an imaginary experiment topologically equivalent to a "Corbino-type" sample of a disk shape with a central hole [16]. Laughlin's arguments were then generalized by Halperin [39] and Büttiker [40] to the strip geometry, employing the properties of the edge states and edge currents. Contemporary understanding of the robustness of the IQHE is based on the topological nature of integer transverse conductivity, first related to Chern numbers by Niu et al. [41] (see also [42] and references therein).

The IQHE requires high, but not extensively high values of the magnetic field, in which several Landau levels are involved. The quantization of the transverse conductivity corresponding to integer values of the filling factor, is of course due to the quantization of the Landau levels. Still, the step-wise behavior of conductivity in the 2D electron gas originates from the influence of impurities [43].

In contrast, in the case of strong magnetic fields in the lowest Landau level regime, the non-interacting particle approach cannot be applied. One can think of the composite-fermion picture in which the fractional filling factor for electrons is transformed into integer filling factors for new quasiparticles: electrons dressed with magnetic quantum fluxes fill completely several Landau levels [44, 45]. However, for this equivalent system of composite fermions in the IQH regime, the role of impurities is strongly combined with effects of interaction. One can think that the impurities play the role of a reservoir of particles trapping or releasing particles as the Fermi level moves across the localized states as the magnetic field changes. Notice that the Fermi energy decreases to lower values as the real magnetic field B grows [16]. As a consequence, for some intervals of B the density of the extended electrons, those that contribute to the current, increases due to the transfer of electrons from impurities to the Landau levels. This effect compensates the increase of B, providing the appearance of a plateau in the resistivity/conductivity:

$$\rho_{yx} \sim B/n_e, \tag{2}$$

where n_e is the density of the extended part of the system. It must be stressed that the presence of impurities plays the same role as that of the edge in finite systems. The main

ingredient is the presence of a scalar potential locally linear in x that traps the particles [16].

The size of the plateaux depends thus on the number and the properties of the impurities. It must be realized that these plateaux appear on special values of ρ_{yx} that localize states of significant interest, with fractional filling factors. Without impurities these values of the resistivity would not be visible.

Turning back to the atomic gases, to simulate the similar phenomenology, we must somehow obtain localized and non-localized particles and look for regimes where transfer between them is possible. Since in ultracold atom setups one has the possibility to engineer controllable impurities, such systems provide an ideal tool to understand the role of impurities in the formation of the plateaux and their interplay with interactions in the FQHE. In our numerical simulations, the possibility of distinguishing localized and non-localized particles was achieved in the following way: The diagonalization of the one-body density matrix provides us with the natural orbitals. Importantly, in all the analyzed cases, one of the orbitals is mostly concentrated around the impurity. In contrast, the other ones remain extended. Therefore we can distinguish between these two parts. Intervals of the artificial magnetic field B^* where the occupations of the natural orbits have a significant variation with B^* turned out to be crucial to identify the regions where transfer is possible and plateaux are expected.

Recently we have used state-of-art exact diagonalization to study properties of small clouds of atoms in a trap under influence of strong artificial gauge fields (see [22, 23, 46, 47, 48, 49, 50, 51]). In this paper, we expand the previous studies [52]. Our main goal is to learn about the relationship between the presence of impurities and the appearance of plateaux in the Hall resistivity as a function of the magnetic field in the fractional quantum Hall regime. This regime has not been achieved experimentally with atoms and our preliminary analysis is intended to predict possible future results. We use here the exact diagonalization method to calculate the ground state (GS) and its excitations in the absence/presence of an impurity. We analyze the time evolution (TE) of the system submitted to a periodic perturbation which represents an applied external electric field to simulate the transport equation

$$j_y(t) = \sigma_{yx} E_x(t) \ , \tag{3}$$

where j_y is the equivalent to the electronic current for atoms and σ_{yx} is the transverse conductivity. In the Appendix we compare the results with those obtained using the linear response theory (LRT) approximation and conclude that, aside some limitations associated with resonances, the comparison is extremely good.

Our main result is the appearance of a plateau close to the GS transition that takes place when the angular momentum changes from $L = N(N-2)$ to $L = N(N-1)$. The change of angular momentum modifies the resistivity and produces a bump partially overlapped with the plateau. An important outcome is that the presence of an impurity is a necessary condition to generate plateaux. With no impurities the change of the occupations is abrupt and the transfer process is not possible.

The numerical complexity of the problem allows us to study only rather small systems up to $N = 4$ atoms. In effect the predicted plateau is small. We expect, however, that for large systems ($N = 100$–1000) the natural increase of the number of impurities and thus the

increase of the localized part, would guarantee the visibility of the plateau. On the other hand, the robustness comes from the topological nature of the conductivity, as previously mentioned.

This paper is organized as follows: In section II we present the model for the basic Hamiltonian H_0 to calculate the full spectrum of the unperturbed system. From its GS, we obtain the natural orbitals and their occupations. In addition, we show the explicit expression of the periodic perturbation and the expression for the equivalent periodic trapping potential in the full Hamiltonian. In section III, we analyze the time evolution of the expected value of the current operator j_y and identify the conductivity. The main results are shown. In section IV we define a kind of restricted operators that emphasize the presence of the plateau and discuss about its meaning. Finally section V contains the summary and discussion. The appendix develops the LRT and shows some comparisons with the TE, as well as some limitations inherently related with the method.

2. The model

We consider a system of N one-component bosonic atoms of mass M confined on the XY-plane. The cloud is trapped by a rotating parabolic potential of frequency $\omega_\perp$ and rotation Ω along the Z-axis, rotation which in an effective way generates an artificial magnetic field denoted by B^*. In the rotating reference frame the basic Hamiltonian (not including the perturbation) reads

$$\hat{H}_0 \;=\; \hat{H}_{\text{sp}} + \hat{H}_{\text{int}}, \tag{4}$$

where the single particle part is given by

$$\hat{H}_{\text{sp}} = \sum_{i=1}^{N} \left[\frac{\hat{\mathbf{p}}^2}{2M} + \frac{M}{2}\omega_\perp^2 \hat{\mathbf{r}}^2 - \Omega \mathbf{z} \cdot \hat{\mathbf{L}} \right]_i + \hat{W} \tag{5}$$

which can be rewritten in an equivalent way as

$$\hat{H}_{\text{sp}} = \sum_{i=1}^{N} \left[\frac{1}{2M}(\hat{\mathbf{p}} + \hat{\mathbf{A}})^2 + \frac{1}{2}M\left(\omega_\perp^2 - \frac{(B^*)^2}{4M^2}\right)\hat{\mathbf{r}}^2 \right]_i + \hat{W} \,, \tag{6}$$

with

$$\hat{A}_x = \frac{B^*}{2}\hat{y} \;,\;\; \hat{A}_y = -\frac{B^*}{2}\hat{x} \,. \tag{7}$$

The particular selection of the symmetric gauge has been done in the definition of $\hat{\mathbf{A}}$, with

$$B^* = 2M\Omega \tag{8}$$

being the modulus of a constant artificial magnetic field directed downward along the Z-direction and $\mathbf{r} \equiv (\mathbf{x}, \mathbf{y})$.

The potential $\hat{W} = \sum_{j=1}^{K} \hat{W}_j$ is due to the presence of K impurities, which are modeled by Dirac delta functions,

$$\hat{W}_j = -\gamma_j \frac{\hbar^2}{M} \sum_{i=1}^{N} \delta^{(2)}(\hat{\mathbf{r}}_i - \mathbf{a_j}) \tag{9}$$
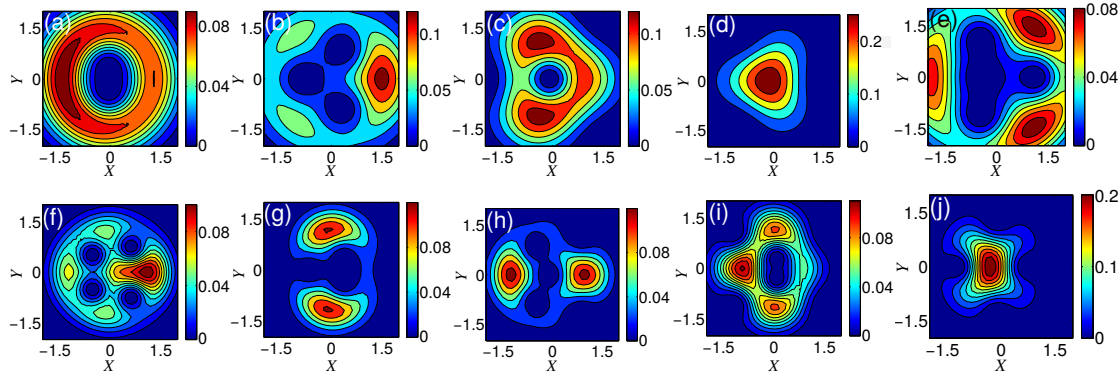
Figure 1. (Color online) Density of the first five natural orbitals, the only ones with non-negligible occupations for $N = 3$ (upper row) and for $N = 4$ (lower row). For $N = 3$, the second one, panel (b), is localized close to the impurity siting at $\mathbf{a_1} = (1, 0)$. In contrast, for $N = 4$, the natural orbital which is localized around the impurity is the first one [panel (f)]. The occupations are: $0.92, 0.74, 0.57, 0.42$ and 0.34 for $N = 3$ and $1.30, 0.83, 0.68, 0.52, 0.41$ and 0.26 for $N = 4$, respectively. In both cases we take $Ng = 6$, $\gamma_1 = 0.1$, $\Omega = 1.95$.

The dimensionless parameters γ_j measure the strength of the impurities and $\mathbf{a_j}$ localize them on the XY plane. The term $\hat{W}$ breaks the circular symmetry except for the case of a single impurity localized exactly at the center.

We model the atomic interaction by a 2D contact potential characterized by

$$\hat{H}_{\text{int}} = \frac{\hbar^2 g}{M} \sum_{i<j} \delta^{(2)}(\hat{\mathbf{r}}_i - \hat{\mathbf{r}}_j), \tag{10}$$

where $g = \sqrt{8\pi} a/\lambda_z$ is the dimensionless coupling, a is the 3D scattering length and $\lambda_z = \sqrt{\hbar/M\omega_z}$. We assume ω_z, the trap frequency in the Z-direction, much larger than any of the energy scales involved, in such a way that only the lowest level is occupied. Therefore, the dynamic is frozen in the Z-axis and the system can be considered two-dimensional.

Without impurities, the solutions of the single particle part produce the Landau level structure [45]. The energy levels are separated by $\hbar(\omega_\perp + \Omega)$. We assume that B^* is large enough to consider just the lowest Landau level (LLL) regime where the appearance of energy gaps has a completely different origin as those in the IQH, where several Landau levels are implied. Within this regime, the kinetic part of the Hamiltonian reads

$$\hat{H}_{\text{kin}} = \hbar(\omega_\perp - \Omega)\,\hat{L} + \hat{N}\hbar\omega_\perp. \tag{11}$$

The single particle solutions with well defined angular momentum m are the Fock-Darwin (FD) functions, given by $\phi_m(\theta, r) = \frac{e^{im\theta}}{\sqrt{\pi m!}} e^{-r^2/2}\, r^m$.

Once the spectrum of the whole system is obtained for a given number of particles N and for fixed values of Ω, γ_j, $\mathbf{a_j}$ and g, we proceed to distinguish the eigenfunctions of the one-body density matrix according to their localization. To this end, we diagonalize the one-body density matrix given by

$$\hat{\rho}^{(1)}(\mathbf{r}, \mathbf{r}') = \langle \hat{\boldsymbol{\Psi}}^\dagger(\mathbf{r}) \hat{\boldsymbol{\Psi}}(\mathbf{r}') \rangle, \tag{12}$$

where the expected value is calculated at the GS and $\hat{\Psi}(\mathbf{r})$ is the field operator. Its eigenfunctions are the natural orbitals ψ_i, linear combinations of the FD functions, and the eigenvalues are their occupations n_i, $i = 1, .., l_m + 1$ (l_m varied until convergence).

From now on, we use the complete set of natural orbitals as a base to represent functions and operators in the second quantized formalism. Next we analyze the density distribution of each orbital and look for their localization around the impurities. For $N = 3$ and one impurity at $\mathbf{a_1} = (\mathbf{1}, \mathbf{0})$ [see Eq. (9) - lengths are in units of the XY harmonic oscillator length], the result is that the orbital ψ_2 out of five orbitals with non-negligible occupation (the orbitals are ordered by decreasing occupations), presents a density distribution mainly localized at the impurity, as is shown in Fig. 1 (upper row). Similar results are obtained for $N = 4$ where the most localized orbital is ψ_1 (lower row). This localization of some orbitals allows us to distinguish between localized and extended states.

Finally, we consider that the cloud of atoms is dynamically forced by an oscillating term, while the impurity remains attached to a fixed position. To be explicit, the full Hamiltonian of the system is

$$\hat{H}(t) = \hat{H}_0 + \hat{H}_{\text{pert}}(t) \tag{13}$$

with

$$\hat{H}_{\text{pert}}(t) = -\lambda \left(\sum_{i=1}^{N} \hat{x}_i \right) \xi(t) \sin(\omega t) \equiv \sum_{i=1}^{N} f(t) \, \hat{x}_i, \tag{14}$$

where λ gives the intensity of the perturbation, which we assume small. The explicit form of $\xi(t)$ is

$$\xi(t) = 1 - \exp[-(t/\sigma)^2] \tag{15}$$

where σ determines the velocity of the evolution. The perturbation is switched on at $t = 0$ and, as t increases, the stationary regime is achieved when the amplitude of the oscillations can be considered constant. From now on we consider $M = 1/2$ and $\hbar = 1$ and choose $\lambda_\perp = \sqrt{\frac{\hbar}{M\omega_\perp}} = \sqrt{2/\omega_\perp}$, $\hbar\omega_\perp/2$ and $\omega_\perp/2$ as units of length, energy, and frequency, respectively. With our unit of length, $\omega_\perp = 2$. In the simulation, the sequence $-\lambda\xi(t)\sin(\omega t)$ is identified with the electric field $E_x(t)$ in the transport equation. Namely, for a single particle and a single impurity [see Eq. (5)], including the perturbation we have

$$\hat{H}_i = (\hat{\mathbf{p}} + \hat{\mathbf{A}})_i^2 + (\omega_\perp^2 - \Omega^2)(\hat{\mathbf{x}}^2 + \hat{\mathbf{y}}^2)_i + f(t)\hat{\mathbf{x}}_i - \gamma_1 \delta^{(2)}(\hat{\mathbf{r}}_i - \mathbf{a_1}). \tag{16}$$

The effective trapping potential can be re-written as an oscillating trap

$$(\omega_\perp^2 - \Omega^2)\left[(\hat{\mathbf{x}} + \frac{f(t)}{2(\omega_\perp^2 - \Omega^2)})^2 + \hat{\mathbf{y}}^2 \right]_i. \tag{17}$$

3. Time evolution

Let us show that this model allows us to identify the transverse conductivity from the transport equation (3). For that, we need to analyze the time evolution of the expected value of the
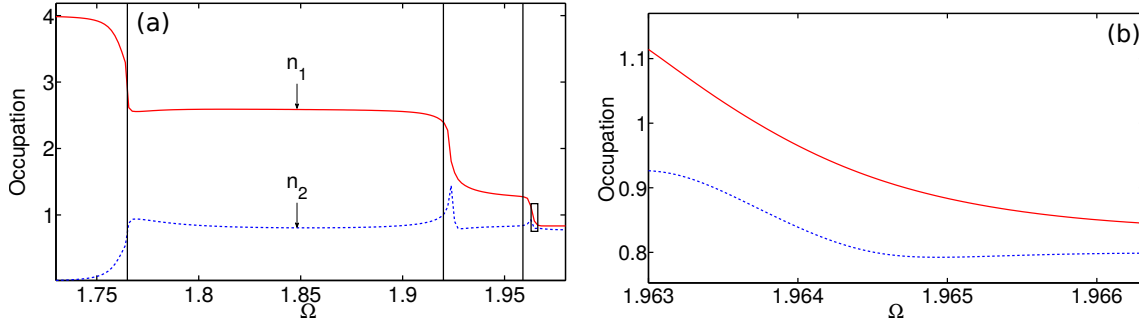
Figure 2. (a) Occupations of the first two orbitals as a function of Ω. There is a correlation between the steps of the occupations and the jumps of $\langle L \rangle$ in a nearly symmetric system. For $N = 4$ the magic numbers of L in the symmetric case are $0 - 4 - 8 - 12$. The vertical lines at 1.765, 1.920 and 1.959 mark the position of the jumps of L for the symmetric case. We considered $N = 4$, $Ng = 6$, $\omega = 1.1$ $\gamma_1 = 0.1$ and $\mathbf{a_1} = (\mathbf{1, 0})$. (b) A zoom in the interesting region [which is highlighted with a small rectangle in (a)]. The localized orbital for $N = 4$ is ψ_1.

current operator $\hat{j}_y$, which is given by [53]

$$
\begin{aligned}
\hat{j}_y(\mathbf{r}) = \frac{1}{2M}\{\hat{\Psi}^\dagger(\mathbf{r}) \left[\hat{\mathbf{p}}_\mathbf{y} + \hat{\mathbf{A}}_\mathbf{y}(\mathbf{r})\right] \hat{\mathbf{\Psi}}(\mathbf{r}) \\
- \left[\left[\hat{p}_y - \hat{A}_y(\mathbf{r})\right] \hat{\Psi}^\dagger(\mathbf{r})\right] \hat{\Psi}(\mathbf{r})\}.
\end{aligned}
\tag{18}
$$

By calculating $\langle \hat{j}_y \rangle_t$ once the stationary regime is reached and *in the case* that we obtain a linear behavior in λ [see Eq. (14)], we are able to obtain the transverse conductivity from the transport equation (3) due to the identification we have done between the perturbation and the electric potential associated with a constant electric field.

To obtain $\langle \Psi(t)|\hat{j}_y|\Psi(t)\rangle$ we solve the Schrödinger equation $i\partial_t\Psi(t) = \hat{H}(t)\Psi(t)$ with the time-dependent Hamiltonian given by Eq. (13). We consider the wave function as $\Psi(t) = \sum_{n=1}^{n_d} c_n(t)\,\Phi_n$ where the set $\{\Phi_n\}$, $n = 1, ..., n_d$ is a basis of the Hilbert space of dimension n_d, given by the many-body wave functions which solve Hamiltonian H_0 with eigenvalues $\{E_n\}$. Then, we obtain the system of equations:

$$
\begin{aligned}
i\partial_t\, c_n(t) = c_n(t)E_n \\
- \lambda\,\xi(t)sin(\omega t)\sum_{m=1}^{n_d} c_m(t) < n|\hat{x}|m >
\end{aligned}
\tag{19}
$$

with the GS(Φ_1) as the initial condition, i.e., $\Psi(t = 0) = \Phi_1$. We solve these equations using the Runge-Kutta fourth-order algorithm. Once we obtain the transverse conductivity σ_{yx}, we can obtain the resistivity from

$$
\rho_{yx} = -\frac{\sigma_{yx}}{|\sigma_{yx}|^2 + |\sigma_{xx}|^2},
\tag{20}
$$

where σ_{xx} is obtained from $j_x = \sigma_{xx}E_x$.

Let us note here that our evolution is rather adiabatic. Indeed, we have checked that the overlap $|\langle\Psi_{GS}|\Psi(t)\rangle|$ remains nearly one at all times. E.g., we numerically obtain that, for
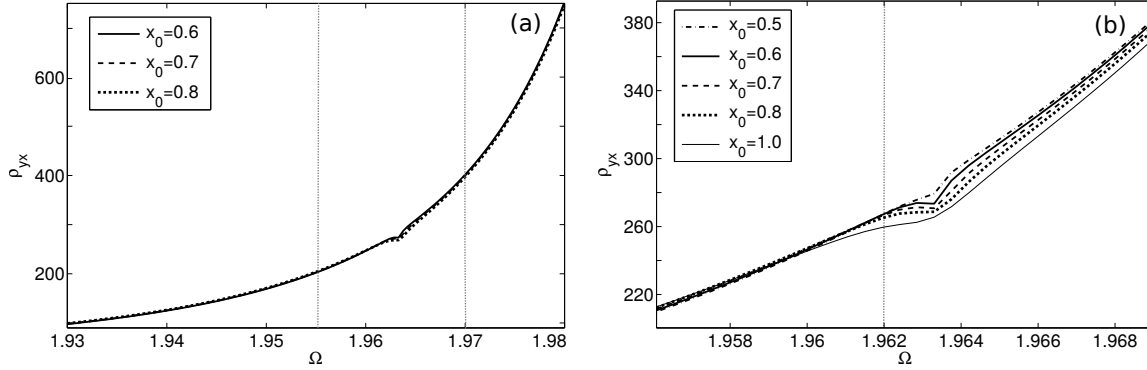
Figure 3. (a) Hall resistivity ρ_{yx} as a function of Ω. We used $N = 4$, $Ng = 6$, $\omega = 1.1$, $\gamma_1 = 0.1$, $\lambda = 0.001$. We considered an impurity at the X-axis at different positions, that is, $\mathbf{a_1} = (\mathbf{x_0}, \mathbf{0})$. The vertical dashed lines mark the interval considered in panel (b), where we show a zoom of the area of interest. The vertical dotted line at 1.962 in panel (b) marks the approximate place of the jump in the angular momentum from 8 to 12. We also include two additional positions of the impurity to show that the effect depends on the position of the impurity.

$\sigma = 10$ (see Eq. (15)),

$$|\langle \Psi_{GS}|\Psi(t_c)\rangle|^2 = 0.97 \tag{21}$$

where Ψ_{GS} is the ground state of $\hat{H}(t_c) = \hat{H}_0 + \hat{H}_{pert}(t_c)$ and $\Psi(t_c)$ is the solution of the Schrödinger equation at t_c (chosen such that $sin(\omega t_c) = 1$).

In agreement with our previous discussion, to generate a plateau we must look for an interval of Ω where the occupation of the localized orbital changes. To this end, we analyze the orbital occupations as a function of Ω [see Fig. 2 (a)] and focus on the region fulfilling two requirements: On one hand, the occupation of the localized orbital decreases as B^* increases producing an increase of the extended part and, on the other hand, this region lies within the largest possible value of $\langle L \rangle$ where plateaux are expected. In other words, there are two kind of intervals: i) intervals where the localized density is flat giving linear dependence of ρ_{yx} with B^* where quantum and classical behavior coincide [16]; and ii) intervals where a plateau occurs and then, the change of B^* drags ρ_d (the extended density), and ρ_{yx} remains constant. Notice that this means that for our analyzed small samples we expect only one plateau along the whole interval of the largest value of $\langle L \rangle$. Fig. 2 (b) is a zoom of the interesting region.

Our main result is represented in Fig. 3, where we show the variation of the Hall resistivity as a function of Ω for some values of the position of the impurity, which we always assume to be in the X-axis, that is $\mathbf{a_1} = (\mathbf{x_0}, \mathbf{0})$. In Fig. 3 (a) we show the Hall resistivity for three exemplary values of the position of the impurity for the whole range of Ω investigated. We observe that some structure, different from the linear behavior, occurs just in the region shown in Fig. 2 (b). This structure begins at about $\Omega = 1.963$, that is just after $\Omega_c = 1.9629$, where the jump of the angular momentum from $L = 8$ to $L = 12$ takes place. In Fig. 3 (b) we show a zoom of the relevant part of the figure, where we confirm that this structure corresponds to the expected plateau. The total jump in the resistivity is for $x_0 = 0.7$ approximately from $\rho_{yx} = 270$ to 291, which is about a 7% of the total value of the resistivity.
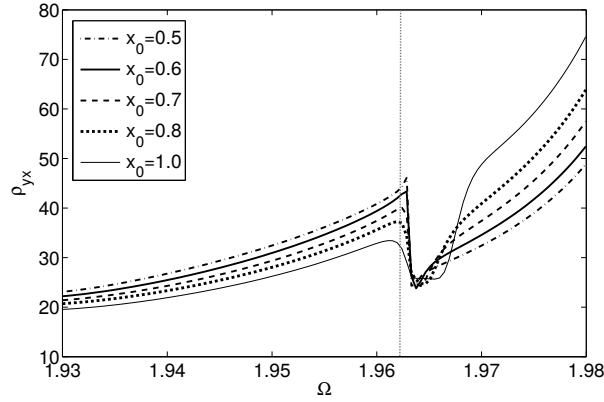
Figure 4. Hall resistivity ρ_{yx} as a function of Ω when restricting both the current and the position operators (see text). Same parameters as in Fig. 3. The presence of a plateau is very evident when using the restricted operators. The plateau begins at about $\Omega = 1.963$ just after $\Omega_c = 1.962$ where the jump of the angular momentum from $L = 8$ to $L = 12$ approximately takes place (marked with a vertical gray dotted line).

We also see that this plateau is soften when the position of the impurity is changed.

4. Emphasizing the plateau structure

Up to this point, it has been proved that the most successful way to generate a plateau is by the localization of a very special interval of Ω where the localized density decreases (see Fig. 2). Within this interval, there is a simultaneous change of B^* and ρ_d. The necessary condition to produce this effect is under the requirement that for each B^*, its "dancing pair", ρ_d, is well defined. To be more precise: For each B^*, the deduction of ρ_{yx} requires several steps, some of them are operations like $\sum_{qp} < q|\hat{j}_y|p >$ or $\sum_{qp} < q|\hat{x}|p >$ where $|p >$ and $|q >$ are Fock states: $|n_1, n_2, ...n_{l_m}\rangle$, n_i being the orbital occupations. In order to have a fixed value of ρ_d the operators $\hat{j}_y$ and $\hat{x}$ must not do significant changes on the localized part.

To be sure that this phenomenology is well captured by our model, we forced the mechanism in an alternative calculation defining a kind of restricted operators $\tilde{j}_y$ and $\tilde{x}$ that fulfill the previous requirement: They do not change the localized part of the density. We consider in the summations only those elements that couple the vectors with the same occupation of the localized orbital (which is n_2 for $N = 3$ or n_1 for $N = 4$). The result shown in Fig. 4 confirms our intuition. Fig. 4 must be compared with Fig. 3(a). The improvement of the visualization of the plateau for some values of x_0 is evident.

Within the intervals of linear dependence of ρ_{yx} with B^* where quantum and classical behavior coincide [16], the use of the restricted operators is irrelevant as the occupation of the localized orbital is flat.

5. Summary and discussion

Within the framework of quantum simulation, we considered a well known effect for electrons under strong magnetic fields. A great amount of experimental data has been accumulated in solid state devices (Ref. [16]) and the most appealing feature lies in the universality of the results. The plateaux of the Hall resistivity as a function of the (strong) magnetic field, obtained for very clean samples yet containing some disorder, signal the presence of peculiar states with well defined fractional filling factors. The values of ρ_{yx} on the plateaux depend only on universal constants ($\hbar$ and e). Up to now, most of these special states still require a challenging explanation not always complete. The translation of this physics to finite systems of atoms and its interpretation is not always easy. As a first attempt, our goal is to understand the mechanism in small samples and try to extrapolate the results to larger systems. Notwithstanding the fact that we can only tackle with small number of atoms, our results can be experimentally tested, given the ability of the new technologies to deal with very small samples and to engineer tunable impurities.

Summarizing, we have obtained a plateau in the Hall resistivity ρ_{yx}/Ω following the expected line of search suggested by the known mechanism in the case of electrons and real fields in the fractional quantum Hall regime. The appearance of a flat region on ρ_{yx} reveals the essence of our goal, namely that there is a transfer of atoms from localized to non-localized atoms as B^* increases. We proved that it is necessary to have part of the system localized around an impurity. The transfer from localized to extended states allows the simultaneous variation of B^* and ρ_d producing a constant value of $\rho_{yx} \sim B^*/\rho_d$ along certain interval of Ω. Particle interaction and the presence of impurities are crucial ingredients, at odds with the case of the integer quantum Hall effect. The improvement of the visualization of the plateau is achieved by forcing the complete exclusion of the localized part, using a restricted version of the operators for the current and the perturbation.

So far we have used the expressions involved in the transport equation, valid for macroscopic systems with uniform density. Namely, the resistivity (or the conductivity) have no space dependence, and the known experimental behavior (see Ref. [54]) is well captured by the linearity of ρ_{yx} against B^* (aside plateau structures or phase transitions of the GS). In contrast, our system is finite and the mean density decreases with B^* producing a non-linear behavior of ρ_{yx} with B^*, which is a finite size effect.

For systems with larger number of particles (several hundreds or thousands of atoms), the presence of impurities represents a small perturbation in the Hamiltonian. Therefore, for large systems with impurities randomly distributed, we do not expect that the plateau depends on the position of the impurities. This is not the case for systems with a small number of atoms, as in this case the presence of the impurities cannot be considered a small perturbation and the plateau depends on the position of the impurity (see Fig. 3). Indeed, the ground state is strongly modified and so is ρ_{yx}, as shown in Fig. 4, with the bump before the plateau in Fig. 4 being due to the presence of the phase transition taking place as the angular momentum jumps from $L = N(N-2)$ to $L = N(N-1)$. The change of angular momentum modifies the resistivity and produces a bump partially overlapped with the plateau.

6. Acknowledgments

Appendix A. Linear response theory

Following the standard protocol to analyze the linear response of a system [55], given an operator $-\lambda \hat{G} f(t)$ simulating a small perturbation (being $\hat{G}$ time-independent) and an operator $\hat{F}$ for a measurable quantity, the dynamical evolution of the expected value of the observable $\hat{F}$ is given by

$$\langle \hat{F} \rangle_t \; - \; \langle \hat{F} \rangle_0 \; = \; \lambda f(t) |\chi(\omega)|, \tag{A.1}$$

where $\chi(\omega)$ has been defined as

$$\chi(\omega) = \sum_{\nu \neq 0} \Big[\frac{\langle 0|\hat{F}|\nu\rangle \langle \nu|\hat{G}|0\rangle}{E_\nu - E_0 + \omega + i\eta}$$

$$+ \frac{\langle 0|\hat{G}|\nu\rangle \langle \nu|\hat{F}|0\rangle}{E_\nu - E_0 - \omega - i\eta} \Big] \equiv |\chi(\omega)| e^{i\delta(\omega)}. \tag{A.2}$$

The sum is extended to all excitations and η is a small quantity.

To obtain information about the Hall response and simulate Eq. (3), connecting with Section II, we make the following choice

$$\hat{G} = \sum_{i=1}^{N} \hat{x}_i, \tag{A.3}$$

$$\hat{F} = \hat{j}_y, \tag{A.4}$$

and

$$f(t) = \xi(t) sin(\omega t), \tag{A.5}$$
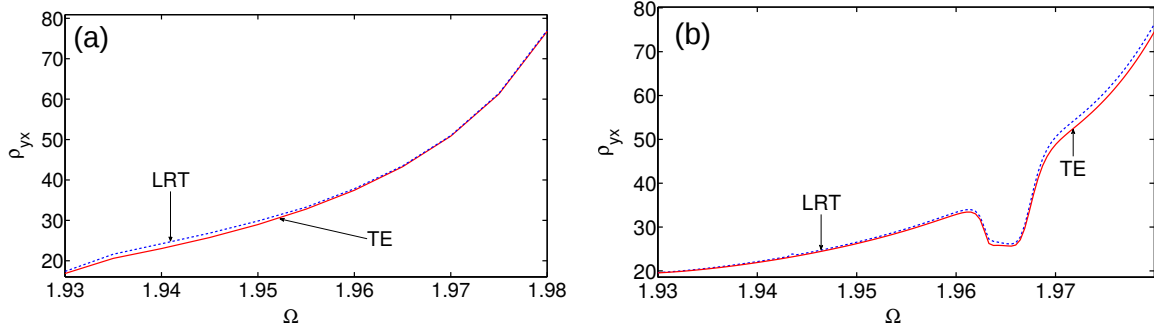
Figure A1. (a) Comparison between the calculation of the Hall resistivity ρ_{yx} as a function of Ω with the complete dynamical evolution (TE) and the result from the LRT for $N = 3$ and $\mathbf{a_1} = (\mathbf{1}, \mathbf{0})$. We use here the restricted operators. Notice that for $N = 3$ within this range of Ω no plateaux occur. (b) same fr $N = 4$ when a plateau is apparent. The figure shows that even in this case, we obtain nearly the same result.
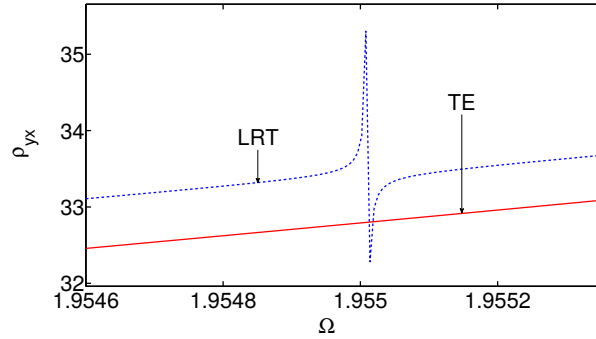

Figure A2. Hall resistivity ρ_{yx} as a function of Ω for $N = 3$ and $\mathbf{a_1} = (\mathbf{1}, \mathbf{0})$. This figure shows a typical resonant structure in the LRT calculation (upper curve) which disappears in the TE case (lower curve).

see Eqs. (14), (15), and (18). If we identify the perturbation with the electric potential associated with a space independent electric field directed along the X-axis,

$$E_x(t) = \lambda f(t) \tag{A.6}$$

then, from Eq. (A.1) it is

$$\sigma_{yx} = |\chi(\omega)| \tag{A.7}$$

and from Eq. (20) we obtain the transverse resistivity ρ_{yx}. The function $\chi(\omega)$ obtained numerically fulfills the condition $\chi^*(\omega) = \chi(-\omega)$ as well as the Kramers-Kronig relations [55].

In what follows we consider three significant results. Fig. A1 (a) shows a comparison between the two techniques: TE and the LRT for ρ_{yx}/Ω. This result indicates that, for a wide range of Ω, the Hall effect is a linear response process. Figure A1 (b) is again a verification that the Hall response is linear even in the case where the response implies the formation of a plateau. Finally, we include Fig. A2 to illustrate possible limitations of the LRT. Notice that the structure of the upper part of Fig. A2 is the typical result of a resonance: For a critical value of Ω and for some excitations, a denominator in the expression of $\chi(\omega)$ [see Eq. (A.2)]

nearly vanishes. The system absorbs energy and the behavior is not linear. Namely the LRT is not applicable there. It could well be a sign of a peculiar state and its Hall response. However, the lower part of the figure demonstrates that this is not the case, that it is not related with the phenomena we are looking for. Notice that Fig. A1 (a) is for $N = 3$, in this case, ρ_{yx}/B^* does not present a plateau, at odds with the result shown in Fig. A1 (b) for $N = 4$ where within the same range of Ω values, a plateau is apparent. In Fig. A1 the LRT result does not show the resonance due to the low resolution.

[1] Y. Imry, *Physics of mesoscopic systems*, in *Directions in Condensed Matter*, G. Grinstein and G. Mazenko Eds. (Singapore, World Scientic, 1986).

[2] Y. Imry, *Introduction to Mesoscopic Physics*, (Oxford University Press, 2002).

[3] M. Lewenstein, A. Sanpera, and V. Ahufinger, *Ultracold atoms in Optical Lattices: simulating quantum many body physics* (Oxford University Press, Oxford, 2012).

[4] M.B. Dahan, E. Peik, J. Reichel, Y. Castin, and C. Salomon, Phys. Rev. Lett. **76**, 4508 (1996).

[5] J. Reeves, B. Gadway, T. Bergeman, I. Danshita, and D. Schneble, New J. Phys. **16**, 065011 (2014).

[6] E. Lucioni, B. Deissler, L. Tanzi, G. Roati, M. Modugno, M. Zaccanti, M. Larcher, F. Dalfovo, M. Inguscio, and G. Modugno, Phys. Rev. Lett. **106**, 230403 (2011).

[7] C. D'Errico, M. Moratti, E. Lucioni, L. Tanzi, B. Deissler, M. Inguscio, G. Modugno, M.B. Plenio, and F. Caruso, New J. Phys. **15** 045007 (2013).

[8] E. Lucioni, L. Tanzi, C. D'Errico, M. Moratti, M. Inguscio, and G. Modugno, Phys. Rev. E **87**, 042922 (2013).

[9] L. Tanzi, E. Lucioni, S. Chaudhuri, L. Gori, A. Kumar, C. D'Errico, M. Inguscio, and G. Modugno, Phys. Rev. Lett. **111**, 115301 (2013).

[10] G. Semeghini, M. Landini, P. Castilho, S. Roy, G. Spagnolli, A. Trenkwalder, M. Fattori, M. Inguscio, and G. Modugno, `arXiv:1404.3528`

[11] J.H. Thywissen, R.M. Westervelt, and M. Prentiss, Phys. Rev. Lett. **83**, 3762 (1999).

[12] S. Krinner, D. Stadler, J. Meineke, J.-P. Brantut, and T. Esslinger, Phys. Rev. Lett. **110**, 100601 (2013).

[13] D. Stadler, S. Krinner, J. Meineke, J.-P. Brantut, and T. Esslinger, Nature **491**, 736 (2012).

[14] J.-P. Brantut, J. Meineke, D. Stadler, S. Krinner, and T. Esslinger, Science **337**, 1069 (2012).

[15] S. Krinner, D. Stadler, D. Husmann, J.-P. Brantut, and T. Esslinger, `arXiv:1404.6400`

[16] D. Yoshioka, *The Quantum Hall Effect* (Springer, Heidelberg, 2002).

[17] R. Prange and S. Girvin, *The Quantum Hall Effect* (Springer Verlag, New York, 1987).

[18] N.K. Wilkin and J.M.F. Gunn, Phys. Rev. Lett. **84**, 6 (2000).

[19] N.R. Cooper, N.K. Wilkin, and J.M.F. Gunn, Phys. Rev. Lett. **87**, 120405 (2001).

[20] B. Paredes, P. Fedichev, J.I. Cirac, and P. Zoller, Phys. Rev. Lett. **87**, 010402 (2001).

[21] M.A. Baranov, K. Osterloh, and M. Lewenstein, Phys. Rev. Lett.**94**, 070404 (2005).

[22] N. Barberán, M. Lewenstein, K. Osterloh, and D. Dagnino, Phys. Rev. A **73**, 063623 (2006).

[23] D. Dagnino, N. Barberán, M. Lewenstein, and J. Dalibard, Nature Phys. **5**, 431 (2009).

[24] T. Grass, M.A. Baranov, and M. Lewenstein, Phys. Rev. A **84**, 043605 (2011).

[25] I. Bloch, J. Dalibard, and W. Zwerger, Rev. Mod. Phys. **80**, 885 (2008).

[26] J. Dalibard, F. Gerbier, G. Juzeliūnas, and P. Öhberg, Rev. Mod. Phys. **83**, 1523 (2011).

[27] N. Goldman, G. Juzeliñas, P. Öhberg, and I.B. Spielman, in print in Rev. Mod. Phys., `arXiv:1308.6533`

[28] M.C. Beeler, R.A. Williams, K. Jiménez-García, L.J. LeBlanc, A.R. Perry, and I. B. Spielman, Nature **498**, 201 (2013).

[29] C.J. Kennedy, G.A. Siviloglou, H. Miyake, W.C. Burton, and W. Ketterle, Phys. Rev. Lett. **111**, 225301 (2013).

[30] M. Aidelsburger, M. Atala, M. Lohse, J.T. Barreiro, B. Paredes, and I. Bloch, Phys. Rev. Lett. **111**, 185301 (2013).

[31] M. Aidelsburger, M. Lohse, C. Schweizer, M. Atala, J.T. Barreiro, S. Nascimbène, N.R. Cooper, I. Bloch, and N. Goldman, `arXiv:1407.4205`

[32] A. Bermudez, N. Goldman, A. Kubasiak, M. Lewenstein, and M.A. Martin-Delgado, New J. Phys. **12**,

033041 (2010).

[33] T. Grass, B. Julia-Diaz, and M. Lewenstein, Phys. Rev. A **86**, 053629 (2012).

[34] R.O. Umucalılar, H. Zhai, and M.Ö. Oktel, Phys. Rev. Lett. **100**, 070402 (2008).

[35] P. Středa, J. Phys. C: Solid State Phys. **15**, L717 (1982).

[36] *The Quantum Hall Effect: Poincaré Seminar 2004*, B. Douçot, B. Duplantier, V. Pasquier, and V. Rivasseau (Eds.), Prog. Math. Phys. **45** (Birkhäuser Verlag, Basel, 2005).

[37] P.W. Anderson, Phys. Rev. **109**, 1492 (1958).

[38] R.B. Laughlin, Phys. Rev. B **23**, 5632 (1981).

[39] B. Halperin, Phys. Rev. B **25** 2185 (1982).

[40] M. Büttiker, Phys. Rev. B **38**, 9375 (1988).

[41] Q. Niu, D.J. Thouless, and Y.-S. Wu, Phys. Rev. B **31**, 3372 (1985).

[42] X.-G. Wen, *Quantum Field Theory of Many-body Systems: From the Origin of Sound to an Origin of Light and Electrons* (Oxford University Press, Oxford, 2007).

[43] R.B. Laughlin, Phys. Rev. Lett. **50**, 1395 (1983).

[44] J.K. Jain, Phys. Rev. Lett. **63**, 199 (1989).

[45] J.K. Jain, *Composite fermions* (Cambridge University Press, Cambridge, 2007).

[46] D. Dagnino, N. Barberán, K. Osterloh, A. Riera, and M. Lewenstein, Phys. Rev. A **76**, 013625 (2007).

[47] B. Julia-Diaz, D. Dagnino, K.J. Günter, T. Grass, N. Barberán, M. Lewenstein, and J. Dalibard, Phys. Rev. A **84**, 053605 (2011).

[48] B. Julia-Diaz, T. Grass, N. Barberán, and M. Lewenstein, New J. Phys. **14**, 055003 (2012).

[49] T. Grass, B. Julia-Diaz, N. Barberán, and M. Lewenstein, , Phys. Rev. A **86**, 021603(R) (2012).

[50] T. Grass, B. Julia-Diaz, and M. Lewenstein, Phys. Rev. A **89**, 013623 (2014).

[51] T. Grass, D. Raventós, M. Lewenstein, and B. Julia-Diaz, Phys. Rev. B **89**, 045114 (2014).

[52] H. Pino, E. Alba, J.Taron, J.J. García-Ripoll, and N. Barberán, Phys. Rev. A **87**, 053611 (2013).

[53] M.J. Edmonds, M. Valiente, G. Juzeliūnas, L. Santos, and P. Öhberg, Phys. Rev. Lett. **110**, 08531 (2013).

[54] R. Willet, J.P. Eisenstein, H.L. Stömer, D.C. Tsui, A.C. Gossard, and J.H. English, Phys. Rev. Lett. **59**, 1776 (1987).

[55] L. Pitaevskii and S. Stringari, *Bose-Einstein Condensation* (Oxford University Press, Oxford, 2003).